Electronic Supplementary Material (ESI) for Materials Horizons.


# Establishing a unified paradigm of microwave absorption inspired by the merging of traditional microwave absorbing materials and metamaterials

*Mengchao Guo, Xiaokun Wang, Haiyan Zhuang, Yuyao Dai, Wei Li, Xuyao Wei, Dongming Tang, Baoshan Zhang, Ping Chen, and Yi Yang* *

*School of Electronic Science and Engineering, Nanjing University, Nanjing, Jiangsu, 210023, China*

*malab@nju.edu.cn

## *Supplementary Material*

Measurement method of EM parameters:

The measurement in 1–18 GHz was performed using coaxial transmission line method. It requires a ring sample whose outer diameter, inner diameter and thickness are 7 mm, 3.04 mm and 2-4 mm, respectively. The ring sample here was obtained by molding the mixture of the FeSiAl powder and paraffin wax. The scattering or S-parameters were measured after putting the ring into the coaxial transmission line that was connected to Agilent N5242A vector network analyzer. On the other hand, the S-parameters can be expressed by the following formula:

$$S_{11} = S_{22} = \frac{i}{2}\left(\frac{1}{z} - z\right)\sin(nk_0 d) \qquad \text{(Equ S1)}$$

$$S_{21} = S_{12} = \frac{1}{\cos(nk_0 d) - \frac{i}{2}\left(z + \frac{1}{z}\right)\sin(nk_0 d)} \qquad \text{(Equ S2)}$$

where $k_0$ is the wave number in vacuum, $d$ is the thickness of the ring, while $n$ and $z$ are the refractive index and impedance of the sample, respectively. Thus, $n$ and $z$ were extracted from the measured S-parameters:

$$n = \pm\frac{1}{k_0 d}\left[\cos^{-1}\left(\frac{1 - S_{11}{}^2 + S_{21}{}^2}{2S_{21}}\right) + 2m\pi\right] \qquad \text{(Equ S3)}$$

$$z = \pm\sqrt{\frac{(1+S_{11})^2 - S_{21}{}^2}{(1-S_{11})^2 - S_{21}{}^2}} \qquad \text{(Equ S4)}$$

Finally, the EM parameters were obtained:

$$\varepsilon = \frac{n}{z} \qquad \text{(Equ S5)}$$

$$\mu = nz \qquad \text{(Equ S6)}$$

Settings of simulation under normal incidence:

The unit structure is modeled in the studio according to Fig. 3(d, e). The measured EM parameters of the composite in 1–18 GHz are imported into CST, according to which the parameters above 18 GHz are automatically fitted by CST. Unit cell, a periodic boundary condition is applied in the x and y directions, with open boundary in the z direction. Frequency Domain Solver is adopted and a plane wave is incident in the –z direction, with the electric field along the y axis.

Settings of Eigenmode simulation:

The unit structure and EM parameters are the same as above. Eigenmode Solver is adopted in CST. Periodic boundary is applied in the x and y directions, with electric boundary in the z direction. The mode electric field distributions take the distributions when the phase shift of one unit is π.

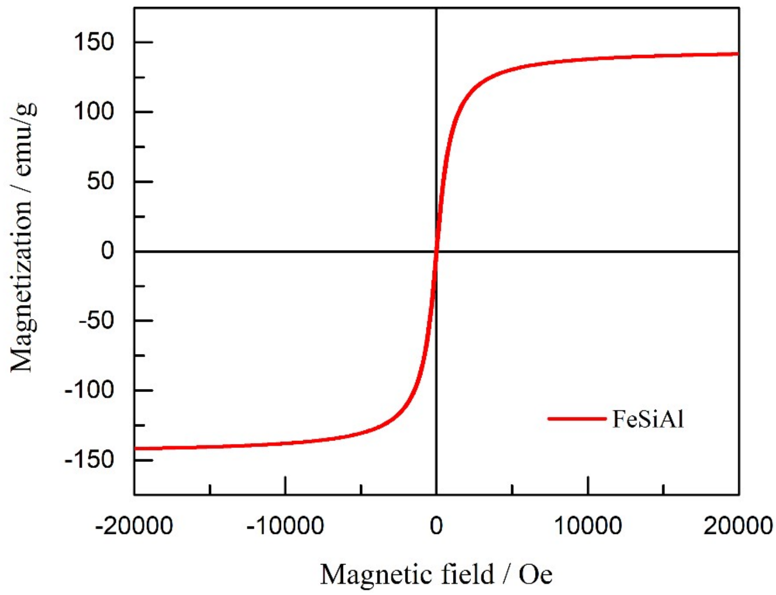


Figure S1. The hysteresis loop of FeSiAl absorbent.

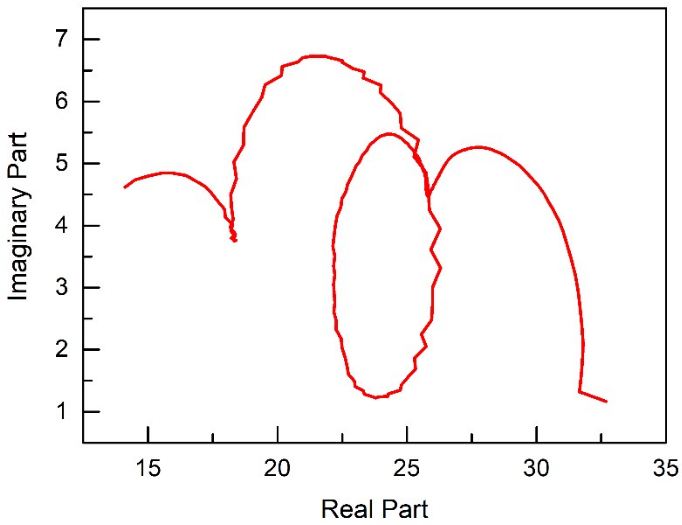


Figure S2. The Cole-Cole curve of the complex permittivity of the FeSiAl-based composite.

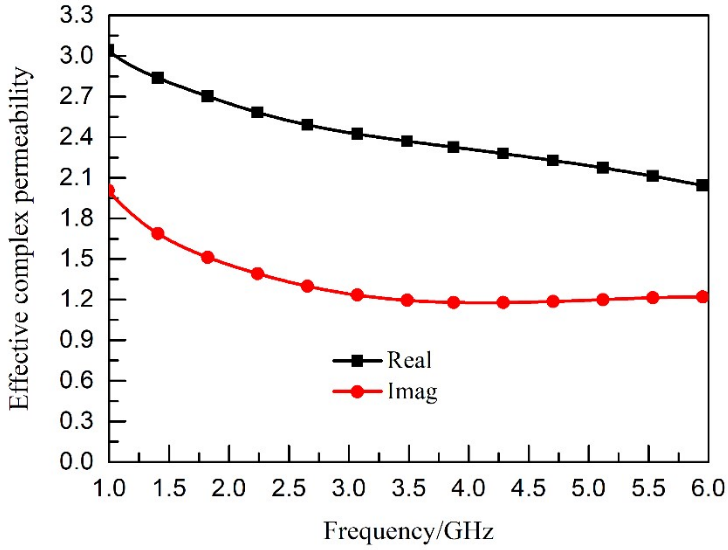


Figure S3. The effective complex permeability of the whole FSMA without the PEC backplane.

To investigate the impedance matching characteristic of the whole FSMA, the input impedance is simulated and shown in Figure S4. It can be seen that the input impedance is close to the impedance of air which is 1-*j*0 in an ultra-wide band especially the imaginary part, indicating good overall impedance matching.

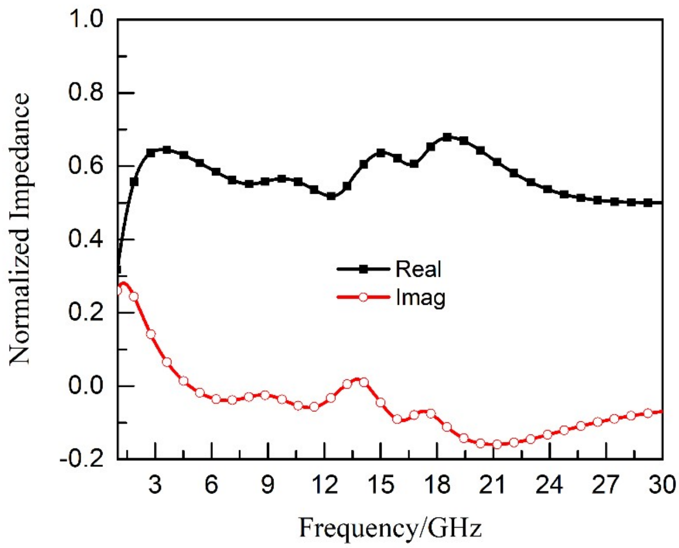


Figure S4. The simulated input impedance.

Besides, the performance without the PEC backplane is also investigated. Figure S5 shows the simulated reflectivity, transmissivity and absorptivity curves without the PEC backplane. It can be found that ultra-broadband absorption can still be realized from 6 GHz to 28 GHz, while the absorptivity decreases rapidly with decreasing frequency in the low frequency range due to the rapidly increasing transmissivity, which can be explained by the necessity of the total reflection property of the PEC backplane to the $\lambda/4$ resonance mechanism in this range. Thus, this FSMA provides wider application range in the circumstances without PEC backplane.

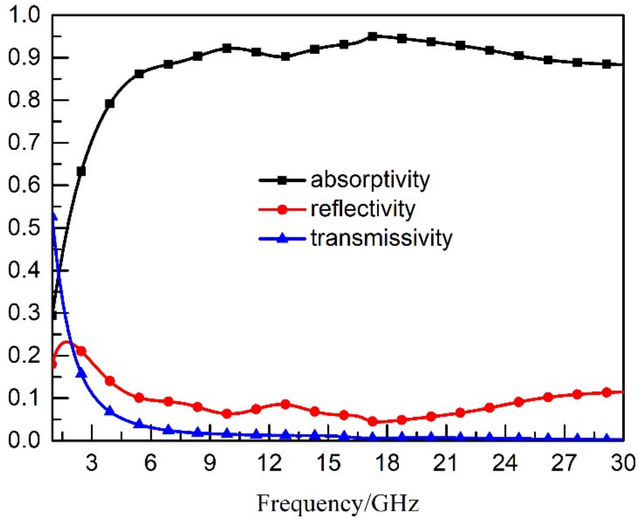


Figure S5. The simulated reflectivity, transmissivity and absorptivity curves without the PEC backplane.

In addition, to investigate whether it has a good performance for oblique incidences, the absorptivity curves under different incident angles for both TE and TM modes are simulated and plotted in Figure S6. For TE mode, the absorption performance is almost unchanged under incident angles within 30 degrees. Even when the incident angle increases to 45 degrees, the absorptivity still remains above 80% from 2GHz to 30GHz. For TM mode, the performance is well maintained under incident angles within 75 degrees. Obviously, this FSMA exhibits an excellent incident angle stability.

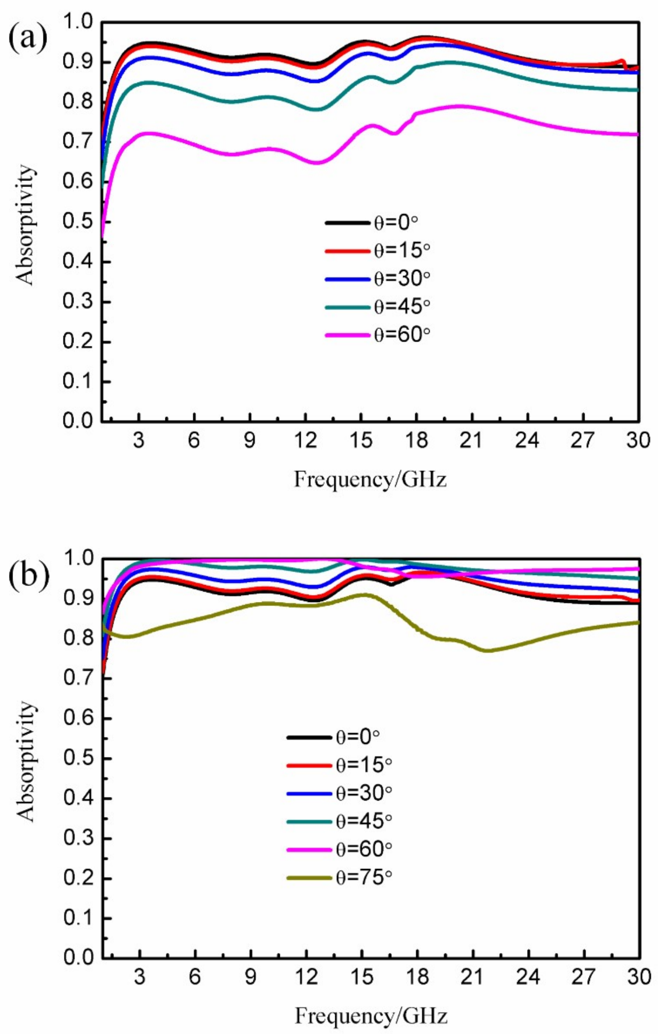


Figure S6. The simulated absorptivity curves under different incident angles for both (a) TE and (b) TM modes.